Solid State Ionics 212 (2012) 1–5

Contents lists available at SciVerse ScienceDirect

Solid State Ionics

journal homepage: www.elsevier.com/locate/ssi

Structural, chemical, and electrochemical characteristics of $LaSr_2Fe_2CrO_{9-\delta}$-based solid oxide fuel cell anodes

Jacob M. Haag [a], David M. Bierschenk [b], Scott A. Barnett [b], Kenneth R. Poeppelmeier [a,*]

[a] Department of Chemistry, Northwestern University, Evanston, IL 60208, USA
[b] Department of Materials Science and Engineering, Northwestern University, Evanston, IL 60208, USA

ARTICLE INFO

Article history:
Received 16 January 2011
Received in revised form 24 January 2012
Accepted 25 January 2012
Available online 5 March 2012

Keywords:
Solid oxide fuel cell
Perovskite
Oxide anode
Redox
Sulfur tolerance

ABSTRACT

Solid oxide fuel cells with $LaSr_2Fe_2CrO_{9-\delta}$–$Gd_{0.1}Ce_{0.9}O_{2-\delta}$ composite anodes were tested in H_2, H_2S-contaminated H_2, and CH_4 fuels as well as under redox cycling conditions. The $La_{0.9}Sr_{0.1}Ga_{0.8}Mg_{0.2}O_{3-\delta}$ electrolyte supported cells had $La_{0.4}Ce_{0.6}O_{2-\delta}$ barrier layers to prevent cation diffusion between $LaSr_2Fe_2CrO_{9-\delta}$ and $La_{0.9}Sr_{0.1}Ga_{0.8}Mg_{0.2}O_{3-\delta}$. After an initial break-in where the performance improved slightly, the cells were stable in humidified H_2 with a power density >0.4 W cm^{-2} and an anode polarization resistance as low as 0.22 Ω cm^2. Anode polarization resistance showed little or no change after 15 redox cycles at 800 °C. Cell performance was stable with 22 ppm H_2S, with only a slight performance decrease relative to pure H_2, but higher H_2S concentrations caused continuous degradation. Also, the performance in humidified CH_4 fuel was quite low.

1. Introduction

The state-of-the-art solid oxide fuel cell (SOFC) anode is Ni-8-mole% yttria stabilized zirconia (YSZ), which performs very well with H_2 fuel. However, Ni–YSZ anodes have a few well-known drawbacks [1]. Ni–YSZ anodes are susceptible to damage by carbon deposition when operated in hydrocarbon-rich fuels. Although such coking can be eliminated by using relatively high steam to carbon ratios, this measure increases system complexity and decreases the efficiency of the SOFC [2]. Ni–YSZ anodes also tend to degrade in fuels containing relatively low levels of common impurities. For example, Ni–YSZ anodes have been reported to undergo irreversible degradation after being exposed to H_2S concentrations as low as 2 ppm at 800 °C [3]. Another issue with Ni–YSZ anodes is redox cycling. Redox cycles can occur when the fuel supply is interrupted, either intentionally or unintentionally [4]. The result can be oxidation of Ni to NiO. The large associated volume increase (69.9%) can lead to fracture or delamination [4], while the subsequent re-reduction can cause Ni to agglomerate, decreasing anode performance [5–8].

A number of doped chromite and titanite solid-solution perovskites have been reported to provide good SOFC anode performance, providing potential alternatives to Ni–YSZ. In some cases, oxide anodes have shown improved functionality compared to Ni–YSZ, including an ability to work stably in CH_4 fuel [6–10], to work without significant poisoning in H_2S-laden fuels [8–11], and to provide stable performance after a number of redox cycles [12]. The $La_{1-x}Sr_xCr_{1-y}Fe_yO_{3-\delta}$ family of perovskites is one of the compositions that has been studied for anode applications. For example, Tao and Irvine reported that $La_{0.75}Sr_{0.25}Cr_{0.5}Fe_{0.5}O_{3-\delta}$ functions as a stable SOFC anode in H_2 fuel, and it is a complete CH_4 oxidation catalyst [9]. A more Fe-rich composition $LaSr_2Fe_2CrO_{9-\delta}$ (LSFeCr) in a composite anode with $Gd_{0.1}Ce_{0.9}O_{2-\delta}$ (GDC) was shown to be stable in H_2 fuel [10] with a polarization resistance of ~0.25 Ω cm^2 at 800 °C, comparable to other oxide anodes. It is also active towards CO oxidation [11].

The present paper discusses a more detailed study of the LSFeCr–GDC anodes. The stability of LSFeCr with $La_{0.9}Sr_{0.1}Ga_{0.8}Mg_{0.2}O_{3-\delta}$ (LSGM) electrolytes and $La_{0.4}Ce_{0.6}O_{2-\delta}$ (LDC) barrier layers was studied. Based on these results, an LDC layer was utilized in the LSGM-electrolyte supported cells to prevent interdiffusion between LSFeCr and LSGM. The electrochemical performance of the composite anodes in humidified H_2 is discussed. Results of electrochemical tests in H_2S-containing H_2 fuel, in CH_4 fuel, and after a number of redox cycles are also described.

2. Experimental

2.1. Synthesis

LSFeCr, LSGM and LDC were synthesized by traditional solid state synthesis from stoichiometric amounts of La_2O_3, $SrCO_3$, Fe_2O_3, Cr_2O_3, Ga_2O_3, MgO and CeO_2 (Alfa Aesar 99.99%). All hydroxides and carbonates were removed from La_2O_3, Ga_2O_3, and MgO by pre-calcining at 800 °C for 4 h. The LSFeCr synthesis was performed at 1250 °C for 24 h typically

* Corresponding author.
E-mail address: krp@northwestern.edu (K.R. Poeppelmeier).

0167-2738/$ – see front matter © 2012 Elsevier B.V. All rights reserved.
doi:10.1016/j.ssi.2012.01.037

with two intermittent grindings. LSGM was calcined at 1250 °C for 6 h and LDC at 1400 °C for 6 h.

2.2. Materials characterization

Structural characterization was performed by powder X-ray diffraction (XRD) using a Scintag XDS 2000 diffractometer with Cu Kα radiation and a nickel filter. Patterns were collected at room temperature in air in the range 20°<2Θ<80° with a 0.02° step size and 1 s dwell.

After verifying phase purity, the chemical compatibility of LSFeCr with different electrolyte materials was studied. LSFeCr was mixed with GDC, LDC and LSGM in a 50%:50% weight ratio and fired at 1000 °C, 1200 °C, and 1400 °C. The mixtures were characterized by powder XRD.

High resolution powder XRD was also performed at the Advanced Photon Source at Argonne National Labs, Beamline 11-BM for the chemical compatibility of LSFeCr and LSGM. LSFeCr and LSGM are similar sized perovskites so high resolution diffraction data was necessary to resolve the highly overlapped diffraction peaks.

2.3. SOFC fabrication

The SOFC testing was performed on LSGM electrolyte supported cells with cathodes consisting of a $La_{0.6}Sr_{0.4}Fe_{0.8}Co_{0.2}O_{3-\delta}$ (LSCF, Praxaiar)–GDC (Nextech) functional layer and an LSCF current collector and anodes comprised of an LSFeCr–GDC functional layer. In most of the cells, an LDC barrier layer was deposited between the anode and electrolyte to prevent reactions between LSFeCr and LSGM [13].

The LSGM powder was ball milled with poly(vinyl butyral-co-vinyl alcohol-co-vinyl acetate) and uniaxially pressed into a 19 mm diameter pellet. The pellets were bisque fired at 1250 °C for 6 h and then an LDC barrier layer was applied to one side of the pellets by either drop coating a colloidal LDC solution or screen printing an LDC ink. The LDC coated pellets were sintered at 1450 °C for 6 h, which resulted in ~400 μm thick, fully dense LSGM pellets and a fully dense LDC layer.

Electrode inks were prepared by ball milling the powders in ethanol for 24 h, drying, and three roll milling with an organic vehicle (Heraeus V737). The anode ink consisted of 50 wt.% LSFeCr and 50 wt.% GDC and was screen printed on the LDC side of the LSGM support. The LSFeCr–GDC active anode layer was fired at 1200 °C for 1–3 h, which resulted in a circular anode active area of 0.28–0.5 cm^2 and a thickness of 30–40 μm. A double layer cathode was used and fabricated by screen printing a 50 wt.% LSCF and 50 wt.% GDC layer on the LSGM support followed by a single phase LSCF layer. The cathode layers were co-fired together at 1000 °C for 3 h (0.5 cm^2 active area, ~20–30 μm thick). Gold ink (Heraeus, Inc) was then screen printed as current collector grids on both electrodes and contacted with silver wires for cell testing. Cross-sectional SEM images of the resulting cells showed the expected structures: dense LSGM with a ~5 μm thick LDC anode layer and a porous anode ~20–30 μm thick.

2.4. SOFC testing

For cell testing, SOFCs were mounted with their anode sides towards alumina support tubes with Ag ink (DAD-87, Shanghai Research Institute of Synthetic Resins). The silver provided both the gas seal and a convenient means for electrically connecting to the anode Au grid. The fuel was provided to the anode through a second, smaller-diameter alumina tube. The setup has been described in more detail elsewhere [14].

Electrochemical measurements were recorded with a four-probe single cell test setup for the current–voltage and electrochemical impedance spectroscopy (EIS, BAS-Zahner IM-6). The electrochemical impedance spectra (EIS) were recorded at open circuit voltage (OCV) over a frequency range of 0.1 Hz to 1 MHz using a 20 mV potential amplitude. The time dependent performance was recorded with a 2420 Keithley Instruments source meter. The anode polarization resistance was estimated as the difference between the low and high frequency real axis intercepts. The cathode contribution to the polarization resistance was negligible based on the relatively low polarization resistances that have been reported for LSCF–GDC cathodes (0.01 Ω cm^2 at 750 °C on YSZ [15] and 0.07 Ω cm^2 at 750 °C on GDC [16] electrolytes).

3. Results and discussion

3.1. Chemical stability and structural characterization

The chemical compatibility of LSFeCr with LSGM and LDC was studied by mixing the powders together and firing from 1000 to 1400 °C. Fig. 1 shows the X-ray powder diffraction patterns of LSFeCr mixed with LSGM after firing at different temperatures. Based on the diffraction patterns, an interaction occurs that becomes more extensive with increasing firing temperature. The inset in Fig. 1 displays the (110) peaks of LSGM and LSFeCr at ~32°. It can be seen that with increasing

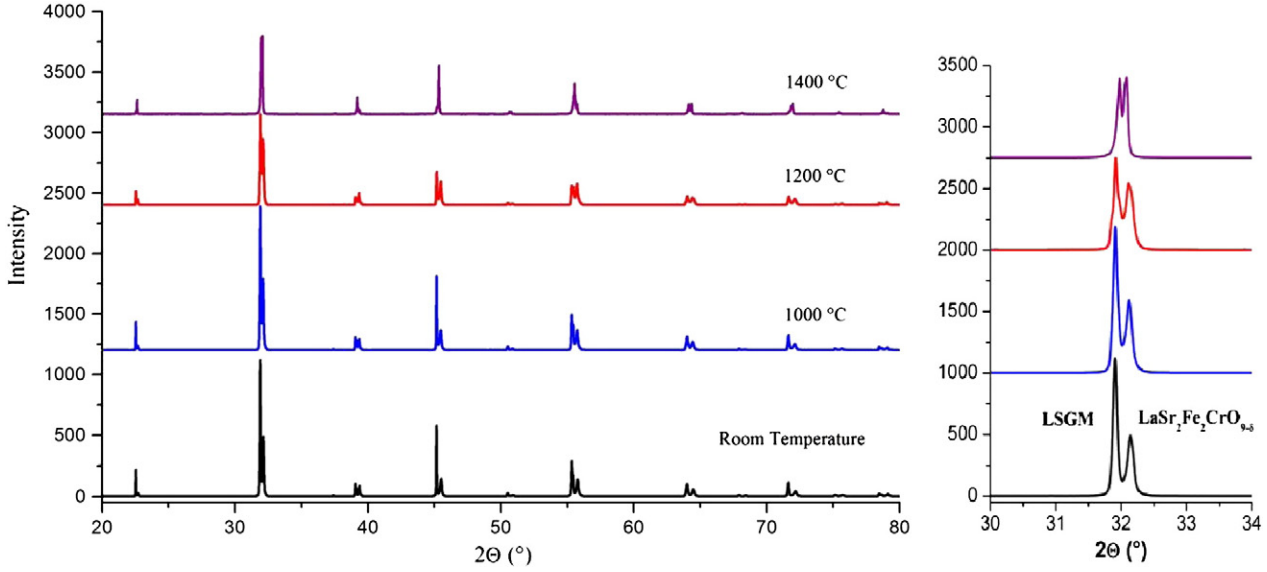

Fig. 1. (a) The XRD patterns of a mixture of LSFeCr and LSGM at room temperature and fired at 1000, 1200, and 1400 °C and (b) an expanded plot of the region between 2Θ 30.5° to 33.5° where the 110 peaks of LSFeCr and LSGM occur.

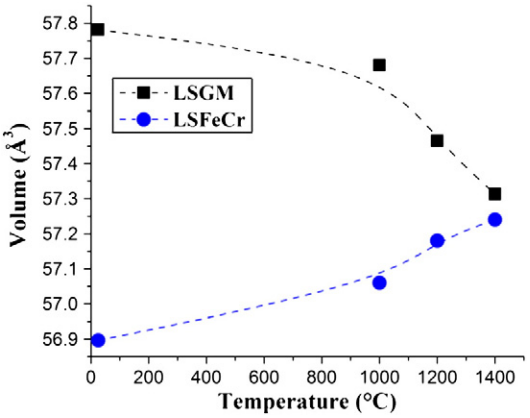

Fig. 2. The reduced unit cell volume of LSFeCr and LSGM at room temperature and after being fired together at 1000, 1200, and 1400 °C.

firing temperature, the (110) LSGM peak shifts to higher 2θ angles indicating a decrease in the volume, while the LSFeCr (110) peak shifts to lower angles signifying an increase in volume. The change in volume is likely caused by the interdiffusion of cations between the two perovskite phases. Fig. 2 shows that the reduced unit cell volumes obtained from the X-ray data converged with increasing firing temperature. This suggests that LSFeCr and LSGM increasingly interdiffused as temperature increased, and would likely form a single phase at sufficiently high temperatures and long times. This agrees with a prior report that a similar composition, $La_{0.75}Sr_{0.25}Fe_{0.5}Cr_{0.5}O_{3-\delta}$, intermixed with LSGM to form a single phase perovskite [17]. This explains why SOFCs with LSFeCr–GDC anodes fired directly on LSGM electrolytes yield low power densities [10]. That is, the mixed phase that forms at the anode/electrolyte interface presumably has inferior electronic or ionic conductivity, and hence has a deleterious effect on the electrode performance.

Fig. 3 shows the X-ray diffraction patterns obtained after firing LSFeCr with LDC. No reaction was observed between LSFeCr and LDC up to 1200 °C. However, after $LaSr_2Fe_2CrO_{9-\delta}$ and LDC were fired at 1400 °C, a significant reaction occurred and a third phase was identified and indexed as the layered perovskite, $LaSrFeO_4$. Thus, LDC provides an effective barrier between LSFeCr and LSGM as long as the firing temperatures were <1400 °C.

LSFeCr is near its stability limit under SOFC anode operating conditions [18]. Detailed studies reported elsewhere showed no evidence of metallic Fe formation under SOFC anode conditions [18], although Fe has been observed when the compound is exposed to highly reducing conditions. In the present work, X-ray diffraction measurements carried out after >100 h SOFC life tests showed only the expected peaks, with no evidence of Fe metal formation.

3.2. Electrochemical testing: hydrogen

All of the SOFCs were initially heated to 800 °C in air and then operated with humidified H_2 (97% H_2–3% H_2O) at the anode, air at the cathode, and a constant applied current until the cell performance stabilized. Cells without the LDC barrier layer exhibited performance that was inconsistent and inferior compared to those with the LDC barrier [10]. All results below were for cells with LDC barriers, which yielded consistent results.

The cells always showed a break-in during the initial 10–20 h of operation where the cell resistance decreased. Fig. 4a shows Nyquist and Bode plots of EIS data measured at open circuit at 800 °C at the beginning of testing (0 h) and after 24 h of operation. Previous impedance data showed that the LSCF–GDC cathodes have a resistance of 0.05 Ω cm^2 at 800 °C [16], with their response centered at ~1000 Hz, a higher frequency than the main impedance response shown in Fig. 4a. Thus, the low frequency response centered at 10 Hz is due to the anode, whereas the small response at ~1000 Hz was due in part to the cathode.

During the initial 24 h of operation, the total resistance of the cell decreased from 0.62 to 0.50 Ω cm^2. Fig. 4 shows that while the ohmic contribution and the high frequency features of the cell impedance were essentially unchanged, the resistance of the low frequency response centered at 1 Hz decreased. This decrease was attributed to changes in anode polarization resistance. $La_{0.8}Sr_{0.2}CrO_{3-\delta}$–GDC anodes have been reported to undergo similar break-in behaviors [19], attributed to the reduction of $La_{0.8}Sr_{0.2}CrO_{3-\delta}$ and the corresponding increase in oxygen ion diffusivity. Therefore, it is possible that the reduction of LSFeCr and the resultant formation of oxygen vacancies [18] increase the ion diffusivity, thereby decreasing the polarization resistance. It is also possible that the surface composition of the LSFeCr is modified during the break-in period, affecting surface reaction kinetics analogous to changes reported for SOFC cathodes [20,21]. Finally, the results indicate that the stable anode polarization resistance was ~0.22 Ω cm^2.

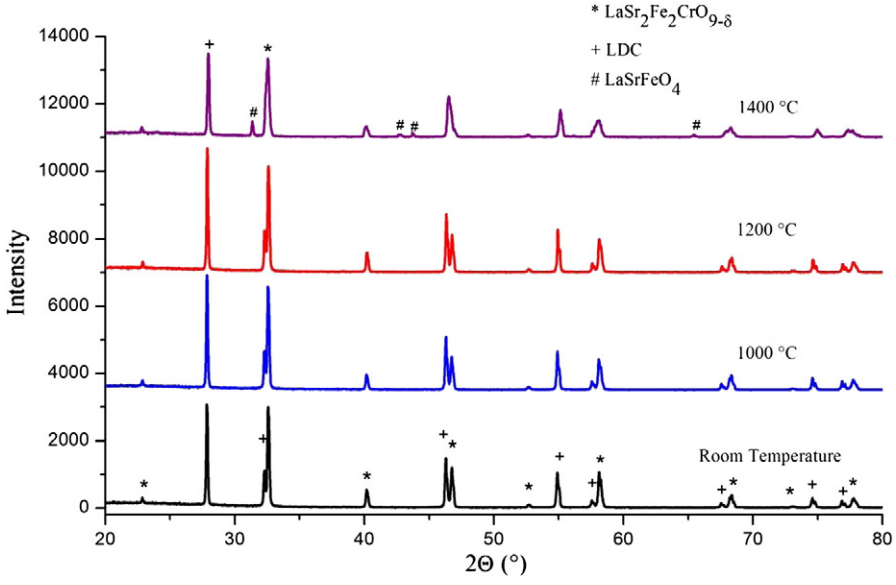

Fig. 3. The XRD patterns of LSFeCr and LDC at room temperature and fired at 1000, 1200, and 1400 °C.

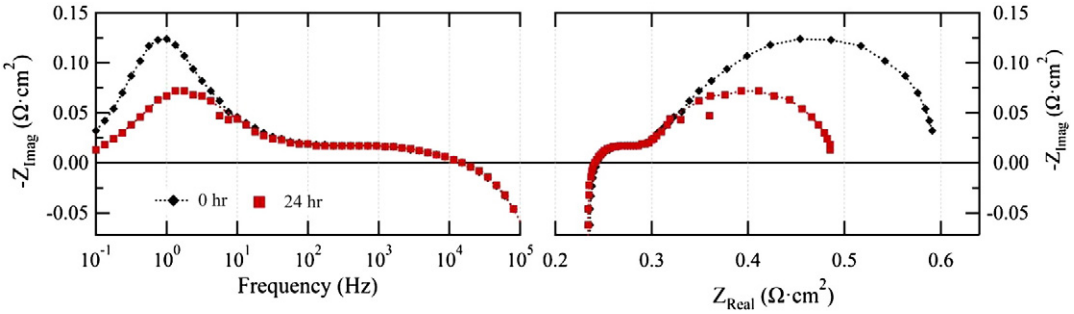

Fig. 4. Bode and Nyquist plots of electrochemical impedance spectra measured for a LSFeCr–GDC anode SOFC at 800 °C at open circuit at 0 h and 24 h of operation.

All measurements described below were done after the break-in period, where the cell performance was quite stable if the humidified H_2 fuel flow was continued. Fig. 5 shows typical current–voltage results, providing a baseline for the tests under different fuel conditions below. Power density at 0.7 V ranged from ~50 mW cm^{-2} at 600 °C to ~400 mW cm^{-2} at 800 °C. The current–voltage curves were approximately ohmic, although there was a slight activated character evident. As shown in Fig. 4, approximately half of the cell resistance was due to the LSGM electrolyte. The cell performance shown here is substantially better than reported previously [10] and is attributed to the LDC barrier layer, which was not used in the prior study.

3.3. Electrochemical testing: redox cycling

Fig. 6 shows the cell voltage versus time during 15 redox cycles, performed after the cell had reached steady state. Each redox cycle involved interrupting the applied current, flushing the fuel lines with Ar, flowing air to the anode for 1 h, resuming the humidified H_2 flow after another Ar flush, and resuming cell operation at 500 mA cm^{-2} for a minimum of 1 h. After each oxidation step, the reintroduction of H_2 fuel led to a rapid recovery in voltage to within ~2% of the initial value. The impedance spectrum at OCV after the 15 redox cycles was nearly identical to that before the cycling, with a ~1% increase in the ohmic resistance and a ~ 1% increase in the polarization resistance. The change was comparable to the slight changes in cell performance normally observed during the cell tests without cycling. Other redox cycles were carried out with oxidation times up to 24 h, but again no change in cell performance was detected. SEM cross sectional images comparing cycled and uncycled anodes showed no indication of microstructural changes or loss of adhesion with the LDC layer attributable to cycling.

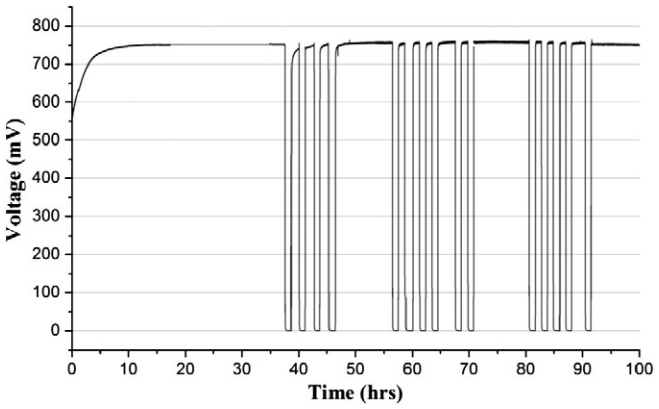

Fig. 6. Voltage versus time for a LSFeCr–GDC anode cell operated on humidified hydrogen at 800 °C. The breaks in the voltage indicate an oxidation cycle.

The redox cycling had no measureable effect on the present anodes, in contrast with results reported for Ni–YSZ anodes with similar thickness. For example, Iwanschitz et. al. observed an increase in the polarization resistance of >100% for 25 μm thick Ni–YSZ anodes after eight 30 min redox cycles at 850 °C [5], and even greater degradation is observed in anode-supported cells due to the much thicker Ni–YSZ layer [6,22].

3.4. Electrochemical testing: sulfur

Fig. 7 shows the cell voltage versus time during operation at 700 mA cm^{-2} and 800 °C with different levels of H_2S contaminant in the humidified H_2 fuel. On switching from pure H_2 to H_2 with

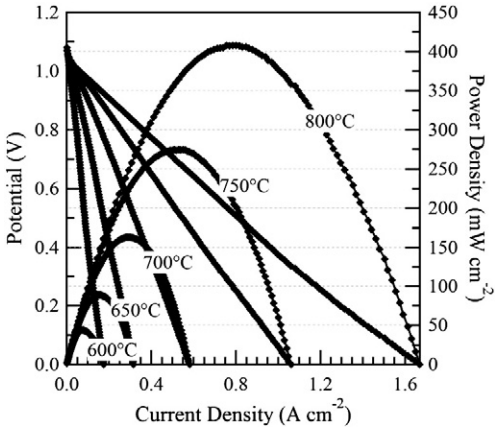

Fig. 5. Potential and power density versus current density, measured in air and humidified hydrogen from 600 to 800 °C, for a typical SOFC.

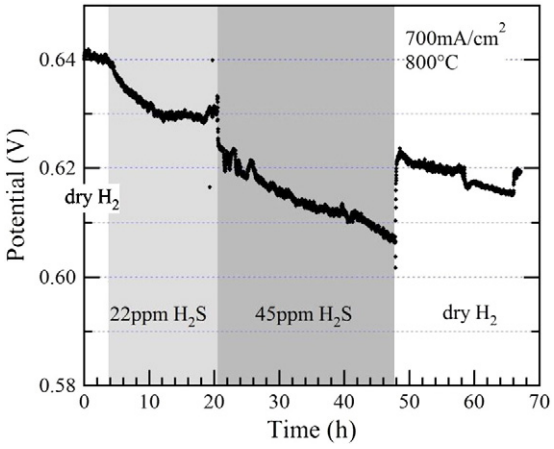

Fig. 7. Cell voltage versus time for an LSFeCr–GDC anode operated on dry H_2 with 22 ppm H_2S, dry H_2 with 45 ppm H_2S, and pure dry H_2.

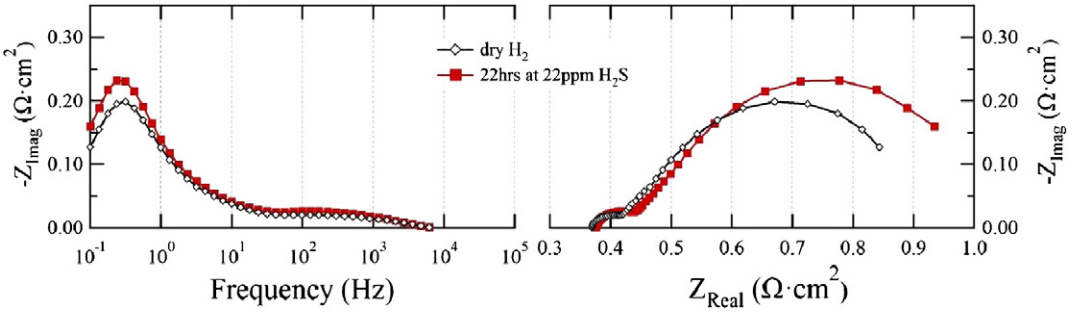

Fig. 8. Electrochemical impedance spectra measured at open circuit for a LSFeCr–GDC anode SOFC at 800 °C expose to 22 ppm H_2S.

22 ppm H_2S, the voltage decreased gradually from 0.64 V to 0.63 V over ~10 h, and then became stable for the subsequent 10 h. That is, the anode was reasonably tolerant to 22 ppm H_2S, reaching a stable voltage only ~3% lower than in pure H_2. At a higher H_2S concentration of 45 ppm, however, there was a small but continuous decrease of 0.5 0m V h^{-1} in cell voltage over the entire 25 h exposure, indicating that the anode was not stable. Upon returning to pure H_2, the voltage partially recovered to 0.62 V, but then continued to decrease gradually. The EIS scans shown in Fig. 8, taken before and during operation in dry H_2 laden with 22 ppm H_2S, again indicate that the changes in cell performance were relatively minor. The Bode plots show that the main effect of H_2S was on the low-frequency response. Increasing the H_2S content to 90 ppm caused significant degradation—the anode polarization resistance increased from 0.4 Ω cm^2 to ~1.6 Ω cm^2 after 55 h of H_2S exposure. Only a fraction of the performance was recovered upon removing the H_2S. These results show better stability and retention of performance than Ni–YSZ anodes [3,23]. For example, for 1 ppm H_2S, there was a 50% increase in Ni–YSZ polarization resistance during operation at 800 °C, larger than that shown here for 22 ppm [23]. Ni–YSZ anodes have been reported to undergo irreversible degradation after being exposed to H_2S concentrations as low as 2 ppm at 800 °C [3]. The results appear to be similar to those reported for other oxide anodes. For instance, Sr_2-$MgMoO_6$ anodes showed a slow but continuous increase in polarization resistance when exposed to 50 ppm H_2S concentration and 800 °C, similar to the present results [24]. $La_{0.75}Sr_{0.25}Cr_{0.5}Mn_{0.5}O_{3-\delta}$ degraded when operated on 0.5% H_2S laden CH_4 at 850 °C [25].

3.5. Electrochemical testing: methane

Cell performance in humidified CH_4 fuel was poor. For example, the cell open circuit voltage dropped to <0.1 V at 800 °C, and the maximum current density that could be drawn was only 165 mA cm^{-2}. This suggests that the present anodes were non-reactive with CH_4–H_2O. That is, there was no reforming activity, because hydrogen produced by reforming would have yielded better cell performance. Hydrogen may also be produced by CH_4 cracking [26], but this did not occur here, as evidenced by the poor cell performance.

4. Summary and conclusions

LSFeCr–GDC composite anodes were tested in LSGM electrolyte-supported cells with an LDC barrier layer to prevent cation diffusion between LSFeCr and LSGM. During an initial break-in, the anode polarization resistance deceased, after which the cell performance was stable in humidified hydrogen with an anode polarization resistance as low as 0.22 Ω cm^2. Impedance spectra showed one main anode feature at relatively low frequency. The redox stability of the LSFeCr–GDC anodes was excellent, with no change in anode resistance, within measurement accuracy, after 15 1 h oxidation cycles at 800 °C. Cell performance in hydrogen with 22 ppm H_2S showed a slight performance decrease relative to pure H_2. Cells operated with 45 ppm degraded continuously at ~0.5 m V h^{-1}. The performance in humidified CH_4 fuel was poor, indicative a low level of reforming activity.

Overall, these anodes are a potential alternative to Ni–YSZ anodes, providing better sulfur tolerance and redox cycling stability, but with higher polarization resistance.

Acknowledgements

The authors gratefully acknowledge the financial support of the Department of Energy (Award No. DE-FG02-05ER46255) and National Science Foundation grant CBET-0854223.

The use of the Central Facilities was supported by the MRSEC program of the National Science Foundation (DMR-0576097) at the Materials Research Center of Northwestern University. The authors would also like to thank Dr. Brian Toby and the 11-BM staff for their assistance with the high resolution X-ray powder diffraction. Use of the Advanced Photon Source at Argonne National Laboratory was supported by the U. S. Department of Energy, Office of Science, Office of Basic Energy Sciences, under Contract No. DE-AC02-06CH11357.

References

[1] A. Atkinson, S. Barnett, R.J. Gorte, J.T.S. Irvine, A.J. McEvoy, M. Mogensen, S.C. Singhal, J. Vohs, Nat. Mater. 3 (2004) 17.
[2] T. Iida, M. Kawano, T. Matsui, R. Kikuchi, K. Eguchi, J. Electrochem. Soc. 154 (2007) B234.
[3] Y. Matsuzaki, I. Yasuda, Solid State Ionics 132 (2000) 261.
[4] D. Sarantaridis, A. Atkinson, Fuel Cells 7 (2007) 246.
[5] D. Fouquet, A.C. Muller, A. Weber, E. Ivers-Tiffee, Ionics 9 (2003) 103.
[6] D. Waldbillig, A. Wood, D.G. Ivey, J. Power Sources 145 (2005) 206.
[7] T. Klemenso, C. Chung, P.H. Larsen, M. Mogensen, J. Electrochem. Soc. 152 (2005) A2186.
[8] B. Iwanschitz, J. Sfeir, A. Mai, M. Schutze, J. Electrochem. Soc. 157 (2010) B269.
[9] S.W. Tao, J.T.S. Irvine, Chem. Mater. 16 (2004) 4116.
[10] J.M. Haag, B.D. Madsen, S.A. Barnett, K.R. Poeppelmeier, Electrochem. Solid-State Lett. 11 (2008) B51.
[11] D.M. Bierschenk, J.M. Haag, K.R. Poeppelmeier, S.A. Barnett, ECS Transactions, 2009, p. 2107, Vienna, Austria.
[12] Q.X. Fu, F. Tietz, Fuel Cells 8 (2008) 283.
[13] K.Q. Huang, J.H. Wan, J.B. Goodenough, J. Electrochem. Soc. 148 (2001) A788.
[14] G.M. Goldin, H. Zhu, R.J. Kee, D. Bierschenk, S.A. Barnett, J. Power Sources 187 (2009) 123.
[15] B.D. Madsen, S.A. Barnett, J. Electrochem. Soc. 154 (2007) B501.
[16] E.P. Murray, M.J. Sever, S.A. Barnett, Solid State Ionics 148 (2002) 27.
[17] J. Pena-Martinez, D. Marrero-Lopez, D. Perez-Coll, J.C. Ruiz-Morales, P. Nunez, Electrochim. Acta 52 (2007) 2950.
[18] J.M. Haag, S.A. Barnett, J.W. Richardson, K.R. Poeppelmeier, Chem. Mater. 22 (2010) 3283.
[19] W. Kobsiriphat, B.D. Madsen, Y. Wang, L.D. Marks, S.A. Barnett, Solid State Ionics 180 (2009) 257.
[20] S.P. Jiang, J.G. Love, J.P. Zhang, M. Hoang, Y. Ramprakash, A.E. Hughes, S.P.S. Badwal, Solid State Ionics 121 (1999) 1.
[21] S. Jiang, J. Mater. Sci. 43 (2008) 6799.
[22] D. Waldbillig, A. Wood, D. Ivey, in SOFC IX, J. Mizusaki, S.C. Singhal, 2005, p. 1244, Quebec City, Canada.
[23] S.W. Zha, Z. Cheng, M.L. Liu, J. Electrochem. Soc. 154 (2007) B201.
[24] J.B. Goodenough, Y.-H. Huang, J. Power Sources 173 (2007) 1.
[25] X.J. Chen, Q.L. Liu, S.H. Chan, N.P. Brandon, K.A. Khor, J. Electrochem. Soc. 154 (2007) B1206.
[26] D. Mogensen, J.D. Grunwaldt, P.V. Hendriksen, K. Dam-Johansen, J.U. Nielsen, J. Power Sources 196 (2011) 25.